Spin dynamics of a Mn atom in a semiconductor quantum dot under resonant optical excitation

S. Jamet, H. Boukari, and L. Besombes[*]

CEA-CNRS group "Nanophysique et semiconducteurs", Institut Néel, CNRS & Université Joseph Fourier,

25 avenue des Martyrs, 38042 Grenoble, France

We analyze the spin dynamics of an individual magnetic atom (Mn) inserted in a II-VI semiconductor quantum dot under resonant optical excitation. In addition to standard optical pumping expected for a resonant excitation, we show that for particular conditions of laser detuning and excitation intensity, the Mn spin population can be trapped in the state which is resonantly excited. This effect is modeled considering the coherent spin dynamics of the coupled electronic and nuclear spin of the Mn atom optically dressed by a resonant laser field. This "spin population trapping" mechanism is controlled by the combined effect of the coupling with the laser field and the coherent interaction between the different Mn spin states induced by an anisotropy of the strain in the plane of the quantum dot.

I. INTRODUCTION

Optically controlled semiconductor quantum dots (QDs) are in many ways similar to atomic systems. In the recent years many quantum optics effects first demonstrated in atoms have been observed on individual QDs. For instance, resonant optical pumping[1] has been successfully used to prepare the spin of an individual electron,[2] hole,[3] or magnetic atom[4] localized in a QD. The possibility of using a strong resonant continuous wave laser field to create hybrid matter-field states[5] and manipulate QDs states in their solid environment has also been demonstrated in different QD systems.[6] The Autler-Townes effect in the fine structure of a neutral or charged QD,[7,8] the Mollow absorption spectrum of an individual QD,[9] and the emission of an optically dressed exciton and biexciton complex[10] have been reported. In magnetic QDs containing an individual Mn atom,[11,12] it has been recently demonstrated that the energy of any spin state of a Mn can be tuned using the optical Stark effect induced by a strong laser field.[13] We present here a way to exploit this coupling with a resonant laser field to initialize the spin of a magnetic atom inserted in a self-assembled QD.

When Mn atoms are included in a II-VI semiconductor self-assembled QD (CdTe in ZnTe),[14] the spin of the optically created electron-hole pair (exciton) interacts with the $5d$ electrons of the Mn (total spin $S = 5/2$). In the case of a singly Mn-doped QD, this leads to a splitting of the once simple photoluminescence (PL) spectrum of an individual QD into six $(2S + 1)$ components.[11,15,16] Since the confined carriers and Mn spin wave functions become strongly mixed, the optical excitation of the QD affects the spin state of the Mn through the exchange interaction offering a possibility of optical control.[4,13,17–20]

The dynamics of the Mn spin at zero magnetic field is mainly controlled by a magnetic anisotropy $\mathcal{D}_0$ produced by the presence of large biaxial strain in the QD plane at the Mn location.[17] This crystal field splits the spin states of the Mn according to $\mathcal{D}_0 S_z^2$. We demonstrated recently the possibility to tune this fine structure using the optical Stark effect.[13] Under strong resonant excitation of a Mn-doped QD optical transition, optically dressed states of the Mn atom are created. The laser-induced energy shift of the optically addressed spin

state can be much larger than the fine-structure splitting of the Mn atom. The laser field can then be used to shift the energy of any spin state of the Mn and control their degeneracy. Here, we present experimental results showing that for particular conditions of laser detuning and intensity, the creation of optically dressed states in a Mn-doped QD can lead to a way to initialize the Mn spin that we call "spin population trapping." We will also model and discuss the parameters that optimize this spin preparation.

This paper is organized as follow: In Sec. II we describe a technique for the readout of the Mn spin state based on a two-photon resonant excitation of an individual Mn-doped QD. In Sec. III we show how the resonant laser excitation on an exciton-Mn (X-Mn) level significantly modifies the Mn spin dynamics. In addition to standard optical pumping expected for a resonant excitation, we show that the spin population can be trapped in the state which is resonantly excited. In Sec. IV we present a model for the spin dynamics of an optically dressed Mn atom and show that it qualitatively explains the experimental results. We demonstrate in particular that the Mn dynamics in the resonant optical excitation regime is strongly affected by the strain anisotropy in the QD plane.

II. TWO-PHOTON READOUT OF THE SPIN STATE OF AN INDIVIDUAL Mn ATOM

The magnetic QDs used in this study are grown on a ZnTe substrate. A 6.5 monolayer thick CdTe layer is deposited at $280\,^\circ\mathrm{C}$ by atomic layer epitaxy on a ZnTe barrier grown by molecular beam epitaxy at $360\,^\circ\mathrm{C}$. The CdTe dots are formed by a high-temperature tellurium-induced process[14] and protected by a 300 nm thick ZnTe top barrier. The QDs are in the 10 nm wide range and a few nm high. Mn atoms are introduced during the CdTe deposition with a density roughly equal to the density of QDs. Nonmagnetic QDs and QDs containing a low number (1, 2,...) of Mn atoms are then formed.

Optical addressing of individual QDs containing magnetic atoms is achieved using microspectroscopy techniques. A high refractive index hemispherical solid immersion lens is mounted on the surface of the sample to enhance the
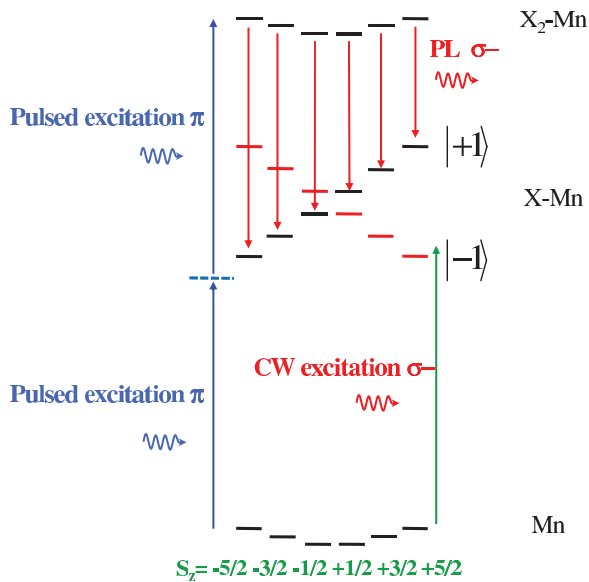
FIG. 1. (Color online) Scheme of the optical transitions and their polarizations in a quantum dot containing an individual magnetic atom and 0 (Mn), 1 (X-Mn), or 2 (X_2-Mn) excitons. The exciton states are split by the exchange interaction with the Mn spin whereas in the ground (Mn) and biexciton (X_2-Mn) states the energy levels results from the fine and hyperfine structure of the Mn spin. A direct resonant excitation of the biexciton is performed by a pulsed two-photon absorption through an intermediate virtual state whereas X-Mn states are resonantly excited by a tunable CW laser.

spatial resolution and the collection efficiency of single-dot emission in a low-temperature ($T = 5$ K) scanning optical microscope.[21]

In order to observe the population repartition on the spin states of the Mn under resonant optical excitation on a given X-Mn level, we developed a technique allowing probing simultaneously the six spin states in the resonant optical excitation regime. The principle of this experiment is presented in Fig. 1. It is based on the creation of a biexciton by a two-photon absorption process under resonant pulsed excitation for the Mn spin readout, combined with a continuous wave (CW) resonant excitation on X-Mn for the Mn spin preparation.

A picosecond pulsed laser excitation tuned between the exciton and the biexciton levels can directly create a biexciton in a QD through a two-photon transition.[23] As the biexciton is a spin singlet state (2 paired electrons and 2 paired holes), in a first approximation it does not interact with the Mn spin.[22] The population distribution on the six Mn spin states is then extracted from the intensity of the PL lines of the biexciton which is controlled by X-Mn in the final state of the biexciton recombination. As the emission of the biexciton is shifted by 10 to 14 meV below the resonant excitation on the X-Mn levels, it can be easily separated from the scattered photons of the CW pumping laser. The resonant two-photon absorption scheme used here also avoids the injection of free carriers in the vicinity of the QD and consequently limits the spin relaxation of the Mn by exchange coupling with these free carriers.[21] Let us note however that the cascade recombination of the biexciton leaves in the QD a maximum of one exciton every
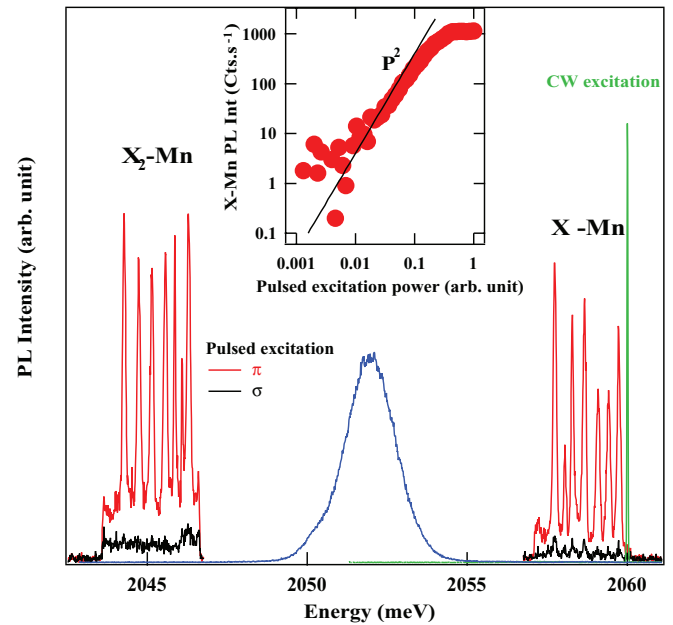

FIG. 2. (Color online) Photoluminescence spectra of a Mn-doped quantum dot (QD1) obtained under a two-photon resonant absorption of a picosecond laser pulse (blue). The resonant creation of the biexciton (X_2-Mn) is only possible for a linearly polarized excitation (red) whereas almost no photoluminescence is observed for circularly polarized pulses (black). The influence on the Mn spin population of a CW control laser (green) in resonance with the exciton (X-Mn) levels can be detected in the intensity distribution of X_2-Mn. Inset: Photoluminescence intensity of one X-Mn line versus the intensity of the pulsed linearly polarized excitation. The P^2 dependence is characteristic of a two-photon absorption.

13 ns (repetition rate of the pulsed excitation). These excitons with a characteristic X-Mn spin-flip time of about 50 ns[4] may slightly perturb the Mn spin preparation. However, as we will see, a signature of the resonant preparation of the Mn is clearly observed in the biexciton signal which appears as a good probe of the Mn spin population.

The experimental evidence of the two-photon resonant formation of X_2-Mn is presented in Fig. 2. As expected from optical selection rules of the two-photon transition,[23] PL from X_2-Mn can only be observed with linearly polarized laser pulses tuned in between the exciton and biexciton transitions. Excitation with circularly polarized pulses does not create any significant QD luminescence. This confirms that one can find experimental conditions where the PL from the QD is dominated by the two-photon resonant excitation. The nonresonant creation of free carriers in the QD vicinity is very weak and will not perturb the Mn spin dynamics.

The intensity distribution of the X_2-Mn created by the two-photon absorption scheme presented above allows us to probe the preparation of the Mn spin by the CW control laser near the resonance with X-Mn states. Such experiments are presented in this paper for three different QDs named QD1, QD2, and QD3. Figure 3 presents the case of QD1 for cross-linear polarization of the resonant CW excitation and the two-photon detection of X_2-Mn. Without CW resonant excitation on X-Mn, an identical intensity is observed for the six main lines of X_2-Mn PL[24] showing that the two-photon excitation does not have any
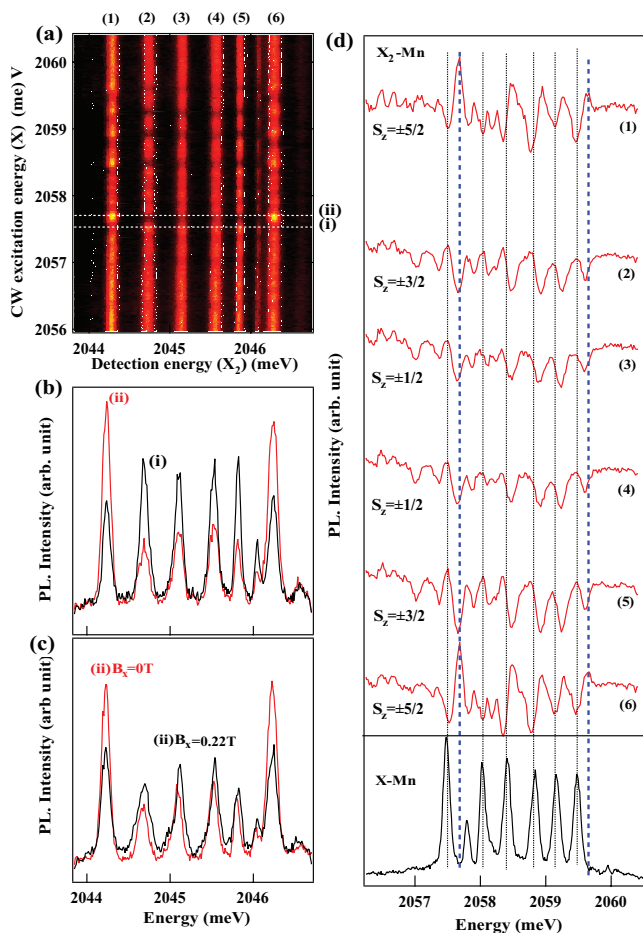
FIG. 3. (Color online) (a) Map of the intensity of X_2-Mn on QD1 versus the energy of the linearly polarized CW resonant excitation on X-Mn for a linearly polarized detection of the two-photon PL of X_2-Mn. (b) PL spectra of X_2-Mn obtained for a resonant CW excitation on (i) and (ii). (c) PL spectra of X_2-Mn under CW excitation on (ii) at zero field (red) and under a transverse magnetic field $B_x = 0.22$ T (black). (d) PL spectra of X-Mn (black) and intensity of each X_2-Mn lines versus the CW laser excitation energy scanned across X-Mn.

significant effect on the Mn spin population. A strong change in the intensity distribution is observed when the CW laser is scanned across each X-Mn level suggesting a complex Mn spin dynamics.

Let us first focus on the two extreme lines in the X_2-Mn PL corresponding to the two degenerate spin states $S_z = \pm 5/2$ (linearly polarized detection). We observe a strong change in the intensity distribution when the CW excitation laser is scanned across the overall structure of X-Mn [Fig. 3(d)]. For instance, each maximum in the intensity of $S_z = \pm 5/2$ occurs with a decrease in the intensity of the other lines associated with $S_z = \pm 3/2$ and $S_z = \pm 1/2$ [dotted blue lines in Fig. 3(d)]. A CW excitation around each X-Mn level produces a modification of the Mn population distribution. For off-resonant excitation, the Mn population is approximately equally distributed on the six spin states.

Figure 3(b) presents two spectra of X_2-Mn obtained when the CW excitation is scanned around the low-energy line of X-Mn $|J_z = \pm 1, S_z = \mp 5/2\rangle$. When the excitation is on

resonance with the low-energy line, the population of $S_z = \pm 5/2$ is weaker than the others: This is the standard optical pumping regime. However, an increase of a few tens of μeV of the excitation energy completely changes the Mn spin population distribution and most of the population can be transferred to states $S_z = \pm 5/2$. PL spectra of X_2-Mn obtained in this excitation regime [(ii) in Fig. 3(a)] with and without transverse magnetic field (i.e., in the QD plane) are presented in Fig. 3(c). A transverse field $B_x = 0.22$ T almost completely restores an equilibrium distribution in the PL intensities of the six lines. This can be explained by the Mn spin precession induced by the transverse field, which completely erases any Mn spin memory. This magnetic field dependence confirms that the observed variations in the two-photon PL of X_2-Mn are linked to the Mn spin population affected by the CW resonant laser. We will now analyze with this detection technique the Mn spin dynamics under resonant optical excitation.

III. Mn SPIN POPULATION REDISTRIBUTION UNDER RESONANT OPTICAL EXCITATION

To address individual Mn spin states, resonant optical experiments are performed under circularly polarized excitation and detection. With circularly polarized photons, an excitation on a given X-Mn level only affects one spin state of the Mn. For co-circular excitation on X-Mn and detection on X_2-Mn, the low-energy lines of X-Mn and X_2-Mn correspond to the same spin state of the Mn (see the level scheme presented in Fig. 1). As presented in Fig. 4, when a CW excitation laser is scanned around the low-energy line of X-Mn, it mainly affects the low-energy line of X_2-Mn. Similarly, as the high-energy line of X-Mn is excited, the intensity of the high-energy line of X_2-Mn is significantly modified. Both configurations show that the resonant CW excitation mainly affects the spin state of the Mn which is resonantly excited.

To analyze the details of the influence of the CW resonant laser on the Mn spin population, we focus on the two outside lines of the PL of X_2-Mn. They correspond to the spin states $S_z = +5/2$ or $S_z = -5/2$. The intensity of these lines is presented in Fig. 4(b) versus the energy of the resonant CW laser. As expected for an optical spin pumping mechanism, one observes a decrease of the $S_z = +5/2$ spin population when the laser is tuned on resonance with the X-Mn level $|J_z = -1, S_z = +5/2\rangle$. However, a strong increase of the $S_z = +5/2$ population is observed when the CW control laser is slightly detuned on the high-energy side of the X-Mn optical transition. A similar behavior is observed when the high-energy line of X-Mn is excited and the high-energy line of X_2-Mn is probed (i.e., exciting and detecting the Mn spin state $S_z = -5/2$). This confirms that, as expected for a Mn spin dependent phenomena, reversing the polarization of detection from co-circular to cross-circular [Figs. 4(c) and 4(d)] reverses the role played by the high and low energy lines of X_2-Mn: An identical strong increase of population is observed on $S_z = +5/2$ or $S_z = -5/2$ for a slightly detuned excitation on the corresponding X-Mn states.

A detail of the evolution of the PL intensity distribution of X_2-Mn obtained by scanning a circularly polarized CW laser around the low-energy line of X-Mn is presented in Fig. 5.
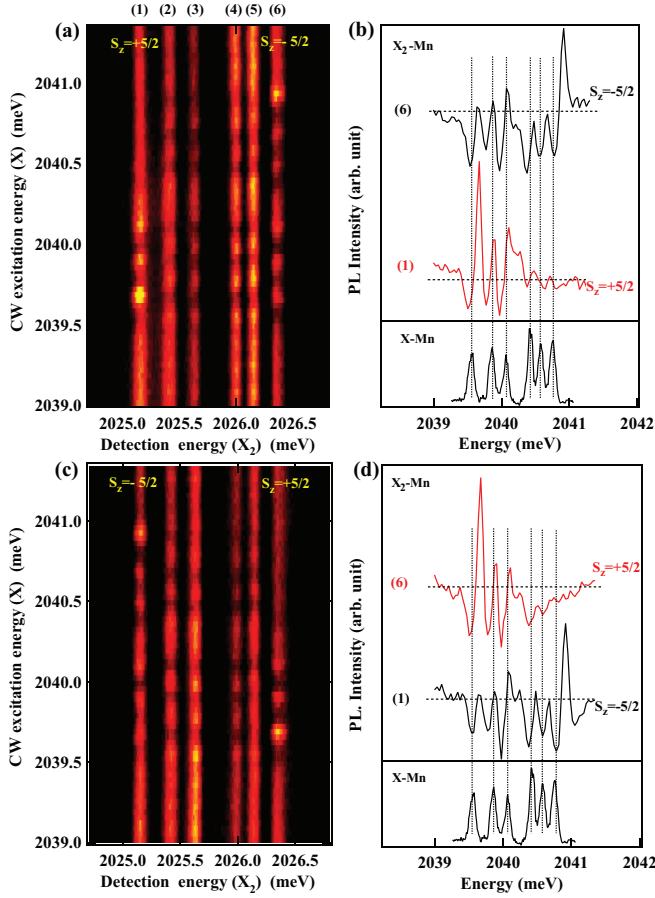
FIG. 4. (Color online) Map of the intensity of X_2-Mn in QD2 versus the energy of the CW resonant excitation on X-Mn for co- (a) and cross- (c) circular CW excitation and detection of X_2-Mn. (b) and (d) present the corresponding intensity curves of X_2-Mn for the spin states $S_z = +5/2$ (1) and $S_z = -5/2$ (6).

FIG. 5. (Color online) High-resolution intensity map of X_2-Mn versus the energy of a single-mode resonant excitation scanned around $|J_z = -1, S_z = +5/2\rangle$ for co- (a) and cross- (c) circular excitation on X-Mn and detection on X_2-Mn (QD2). (b) and (d) present the corresponding intensity curves of X_2-Mn for the spin states $S_z = -5/2$ and $S_z = +5/2$.

These scans allow us to quantify the energy shift needed to optimize the Mn spin preparation. A maximum of the $S_z = +5/2$ spin population is obtained for a laser detuning of about 60 μeV when the excitation is scanned on the low or high energy line of X_2-Mn in co- or cross-circular polarization, respectively.

These experimental results show that the resonant CW excitation decreases the population of the spin state which is resonantly excited as expected from previous resonant optical pumping experiments.[4] More surprisingly, a slight detuning of the resonant CW laser increases significantly the Mn spin population in the state which is optically addressed. We will see in the following that this "spin population trapping" is a specific signature of the coherent dynamics of the Mn spin coupled with its nuclear spin and the resonant laser field.

IV. DYNAMICS OF A Mn ATOM UNDER A RESONANT LASER FIELD

To model the influence of a resonant laser field on the spin dynamics of a Mn atom embedded in a QD, we start from the analysis of the spin structure of a Mn atom in a strained zinc-blende semiconductor matrix. The Hamiltonian
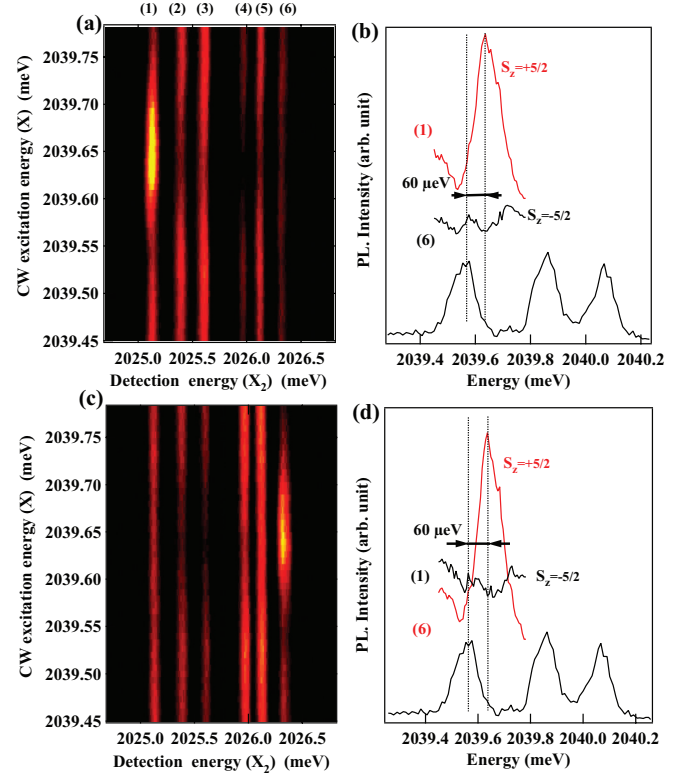
of the coupled electronic and nuclear spins of a Mn atom in a strained layer grown along [001] axis is known from magnetic resonance measurements[26] and reads

$$
\begin{aligned}
\mathcal{H}_{\mathrm{Mn}} = {} & \mathcal{A}\vec{I} \cdot \vec{S} \\
& + \tfrac{1}{6}a\left[S_x^4 + S_y^4 + S_z^4 - \tfrac{1}{5}S(S+1)(3S^2+3S-1)\right] \\
& + \mathcal{D}_0\left[S_z^2 - \tfrac{1}{3}S(S+1)\right] + E\left[S_x^2 - S_y^2\right] \\
& + g_{\mathrm{Mn}}\mu_B\vec{B}\cdot\vec{S},
\end{aligned} \tag{1}
$$

where $\mathcal{A}$ is the hyperfine coupling ($\mathcal{A} \approx +0.7\ \mu$eV),[27] which results from the magnetic dipolar interaction between the Mn $5d$ electrons forming the total spin $\vec{S}$ and the spin of the Mn nucleus $\vec{I}$ ($I = 5/2$). The second term of the Hamiltonian comes from the cubic symmetry of the crystal field and mixes different S_z of the Mn spin. We have $a = 0.32\ \mu$eV according to Ref. 25.

The presence of biaxial strains in the QD plane leads to the magnetic anisotropy term with $\mathcal{D}_0 \approx 12\ \mu$eV for a fully strained CdTe layer matched on a ZnTe substrate. Because of partial relaxation of the strain during the growth process, weaker values of $\mathcal{D}_0$ are usually observed in self-assembled QDs.[17] An anisotropy of the strain in the xy plane (QD plane) can mix different S_z components through the anisotropic crystal field. This coupling is described in the Hamiltonian (1) by its characteristic energy E which depends on the local strain distribution at the Mn atom location.
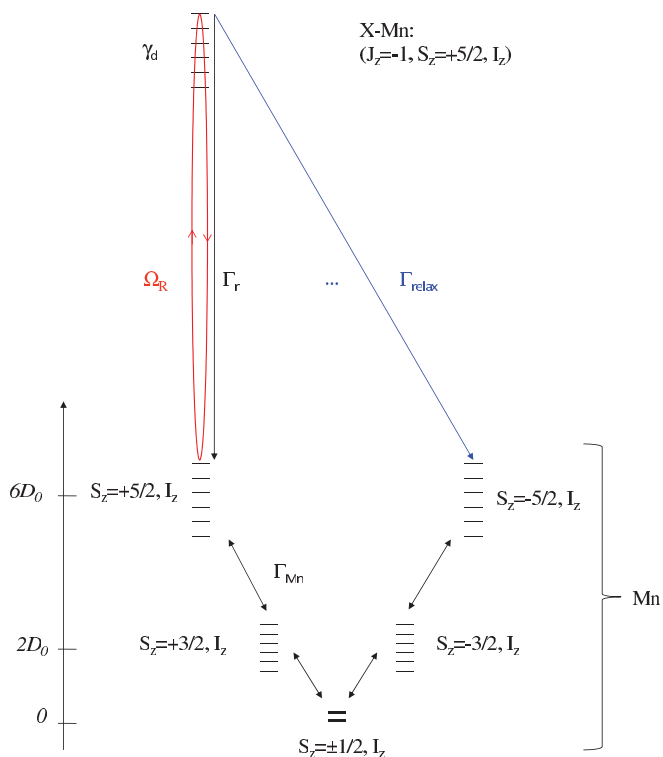
FIG. 6. (Color online) Scheme of the energy levels and transition rates involved in the resonant excitation model (see text). $\hbar\Omega_R$ is the energy coupling with the laser, $\gamma_d = 1/\tau_d$ is a pure dephasing rate of the exciton, $\Gamma_{Mn} = 1/\tau_{Mn}$ is the spin relaxation rate of the Mn, $\Gamma_r = 1/\tau_r$ is the optical recombination rate of the exciton. A relaxation rate of the exciton-Mn complex $\Gamma_{relax} = 1/\tau_{relax}$ is used for an effective description of the optical pumping effect.

In highly strained QDs at zero magnetic field, the Mn electronic spin is quantized along the growth axis z and the different electronic spin doublets ($S_z = \pm 1/2$, $S_z = \pm 3/2$, and $S_z = \pm 5/2$) are separated by an energy proportional to $\mathcal{D}_0$ (Fig. 6). The $S_z = \pm 5/2$ and $S_z = \pm 3/2$ doublets are split into six lines by the hyperfine coupling with the nuclear spin $I = 5/2$. For the doublet $S_z = \pm 1/2$, the isotropic coupling with the nuclear spin $I = 5/2$ results in two levels with total spin $M = 2$ and $M = 3$. The regular spacing between the electronic spin levels can be restored by a magnetic field $B \geqslant 0.5$ T [last term of Hamiltonian (1)].

Different S_z of the Mn are coupled by the nondiagonal terms of H_{Mn} [Eq. (1)]. For instance, the hyperfine terms $\mathcal{A}$ couples two consecutive Mn spin states through an electron-nuclei flip-flop. We could then expect that a nonequilibrium population of the electronic spin prepared optically would be transferred to the nuclear spin. This would lead to an optical pumping of the nuclear spin of the Mn. However, in the presence of a large magnetic anisotropy, these electron-nuclei flip-flops are blocked.

An anisotropic strain distribution in the QD plane can also efficiently couple Mn spin states S_z separated by two units through the crystal field term $E(S_x^2 - S_y^2)$. As we will see, all these coupling terms affect the population redistribution on the six Mn spin states under resonant optical pumping.

The coupling with a resonant laser field can be used to tune the energy of one selected Mn spin state across the full fine structure of the Mn atom.[13] This allows in particular restoring the degeneracy of two consecutive Mn spins states giving an optical way to control the flip-flops of the electronic and nuclear spins. The energy tuning of the optically dressed states is then expected to influence the dynamics of the coupled electronic and nuclear spins. To estimate this effect, we calculated the coherent evolution of coupled electronic and nuclear spins optically coupled to an X-Mn state.

As illustrated in Fig. 6, we first consider that a single exciton state ($|J_z = -1\rangle$) is laser coupled to one state of the Mn ($|S_z = +5/2, I_z\rangle$) with a Rabi energy $\hbar\Omega_R$. This approximation is justified in strongly confined QDs with a large X-Mn splitting resonantly excited by a narrow-band laser and in the limit of small laser detuning. The exciton has a pure dephasing rate γ_d and the relaxation of the Mn spin in the ground state (empty QD) is described by a relaxation rate Γ_{Mn} coupling one by one the different electronic spin states S_z. The nuclear spin I_z is considered to be frozen in the timescale of all the spin preparation mechanism discussed here.

The X-Mn complex can relax its energy along a Mn spin conserving channel at rate Γ_r (optical recombination of X) or along channels including a relaxation of the Mn spin at rate $\Gamma_{relax} = 1/\tau_{relax}$: Γ_{relax} allows a transfer of population from the state $|J_z = -1, S_z = +5/2, I_z\rangle$ to any other spin state of the Mn S_z with I_z unchanged. This is a simplified effective way to describe the complex X-Mn spin dynamics at the origin of the optical pumping mechanism.[28,29] At magnetic fields lower than a few hundred mT, we also consider that the Zeeman energy of the X-Mn can be neglected since it is much smaller than the X-Mn exchange interaction: We only take into account the effect of the magnetic field on the empty QD [last term of Hamiltonian (1) for a Mn alone].

Using the simplified level scheme presented in Fig. 6, we can calculate the time evolution of the 42×42 density matrix ϱ describing the population and the coherence of the 36 states of the Mn alone (empty QD described by $\mathcal{H}_{Mn}$) and the 6 X-Mn states $|J_z = -1, S_z = +5/2, I_z\rangle$. The master equation which governs the evolution of ϱ can be written in a general form (Lindblad form) as

$$\frac{\partial \varrho}{\partial t} = -i/\hbar[\mathcal{H}, \varrho] + L\varrho. \quad (2)$$

$\mathcal{H}$ is the Hamiltonian of the complete system (Mn and X-Mn) and $L\varrho$ describes the coupling or decay channels resulting from an interaction with the environment.[30] One can split $L\varrho$ in three parts:

(1) The population transfer from level j to level i in an irreversible process associated with a coupling to a reservoir is described by $L_{inc, j \to i}\varrho$:

$$L_{inc, j \to i}\varrho = \frac{\Gamma_{j \to i}}{2}(2|i\rangle\langle j|\varrho|j\rangle\langle i| - \varrho|j\rangle\langle j| - |j\rangle\langle j|\varrho), \quad (3)$$

where $\Gamma_{j \to i}$ is the incoherent relaxation rate from level j to level i. This operator describes the radiative decay of the exciton (irreversible coupling to the photon modes) or the relaxation of the Mn spin (irreversible coupling to the phonon modes). Such term could also be used to describe the optical generation of an exciton in the low-excitation regime where

the energy shift induced by the strong coupling with the laser field is neglected.

(2) A pure dephasing (i.e., not related to an exchange of energy with a reservoir) is also introduced for the exciton and described by $L_{\mathrm{deph},jj}\varrho$:

$$L_{\mathrm{deph},jj}\varrho = \frac{\gamma_{jj}}{2}(2|j\rangle\langle j|\varrho|j\rangle\langle j| - \varrho|j\rangle\langle j| - |j\rangle\langle j|\varrho), \quad (4)$$

where γ_{jj} is a pure dephasing rate.

(3) For a general description, valid from the low to the high optical excitation intensity regime, we consider that the laser field induces a coherent coupling between the ground and exciton states. The coherent coupling between two levels induced by the laser field leads to Rabi oscillations between the populations ϱ_{ii} and ϱ_{jj} and coherence of these levels $\varrho_{ij} = \varrho_{ji}^*$. In the Lindblad equation (2), this reversible coupling can be described by $L_{\mathrm{coh},i\leftrightarrow j}$:

$$L_{\mathrm{coh},i\leftrightarrow j}\varrho = i\frac{\Omega_{ij}}{2}(|j\rangle\langle i|\varrho + |i\rangle\langle j|\varrho - \varrho|j\rangle\langle i| - \varrho|i\rangle\langle j|),$$

$$(5)$$

where $\hbar\Omega_{ij} = \mathcal{P}_{ij}\mathcal{E}$ is the Rabi energy splitting with $\mathcal{P}_{ij}$ the dipolar moment of the QD transition and $\mathcal{E}$ the amplitude of the electric field of the resonant CW laser. This term, which corresponds to the dipole-field coupling $-\vec{\mathcal{P}}_{ij} \cdot \vec{\mathcal{E}} = -\hbar\Omega_{ij}(|j\rangle\langle i| + |i\rangle\langle j|)/2$, could also be included in the Hamiltonian evolution [first term of Eq. (2)].[30,31]

The calculated evolution of the population of the different spin states of the Mn with the detuning of a circularly polarized laser around $|J_z = -1, S_z = +5/2, I_z\rangle$ is presented in Fig. 7 for different Rabi energies. The detuning δ is defined as $\delta = \hbar\omega_0 - \hbar\omega_l$ with $\hbar\omega_0$ the energy of the optical excitonic transition and $\hbar\omega_l$ the energy of the CW laser.[30] The states $|S_z = +5/2, I_z\rangle$
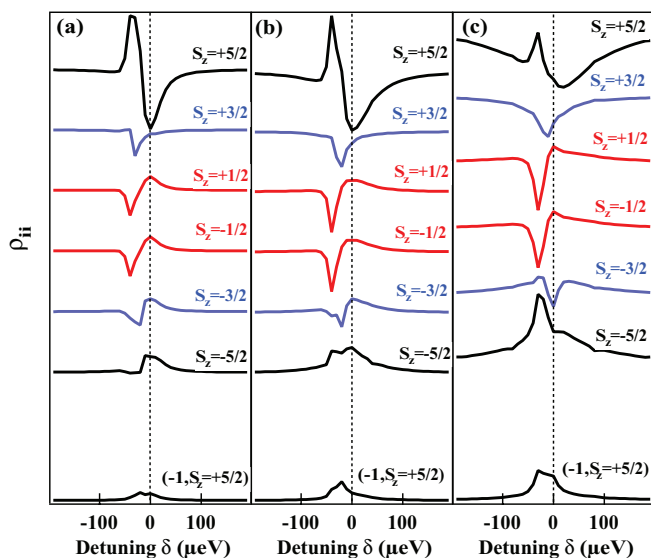

FIG. 7. (Color online) Calculated population of the six electronic spin states of a Mn versus the detuning δ of the CW control laser around the X-Mn state $|J_z = -1, S_z = +5/2, I_z\rangle$ for different Rabi energies: (a) $\hbar\Omega_R = 12.5\ \mu$eV, (b) $\hbar\Omega_R = 25\ \mu$eV, and (c) $\hbar\Omega_R = 50\ \mu$eV. The relaxation times are $\tau_{\mathrm{Mn}} = 250$ ns, $\tau_r = 0.25$ ns, $\tau_{\mathrm{relax}} = 60$ ns, $\tau_d = 100$ ps, and the Mn fine-structure parameters $\mathcal{D}_0 = 7\ \mu$eV and $E = 0.35\ \mu$eV.

of the Mn are coupled by the CW resonant laser to the X-Mn states $|J_z = -1, S_z = +5/2, I_z\rangle$ and we neglect the possible excitation of more than one exciton state by the resonant laser (i.e., the splitting between the X-Mn lines is larger than the Rabi energy or the detuning of the laser). At low Rabi energies and zero detuning, a strong decrease of the population of $S_z = +5/2$ and an increase of the population of the other spin states is observed: This corresponds to the expected optical pumping of the state $S_z = +5/2$. As the laser is slightly detuned on the high-energy side of the transition, $\delta < 0$, a strong increase of the $S_z = +5/2$ population and simultaneous decrease of the $S_z = \pm1/2$ population is observed. This detuning dependence, which we call "spin population trapping," is very similar to the experimental data.

The calculation shows that the states $S_z = +5/2$ (excited by the CW resonant laser) and $S_z = \pm1/2$ are the most affected by the laser detuning [see for instance Fig. 7(b)]. Let us give a qualitative description of the observed complex spin dynamics. As the CW laser is detuned on the high-energy side of the transition, the optically dressed states associated with $S_z = +5/2$ can be pushed on resonance with $S_z = \pm1/2$. At resonance, mixed states of $S_z = +1/2$ and $S_z = +5/2$ are created through the anisotropic crystal field [E term of Eq. (1)]. This coherent coupling produces an enhancement of the population transfer between $S_z = +1/2$ and the optically dressed states associated with $S_z = +5/2$.

The optical recombination of the optically dressed state, which is mainly an excitonic state, induces an irreversible transfer of population from $S_z = +1/2$ to $S_z = +5/2$. In addition, $S_z = +1/2$ and $S_z = -1/2$ are coherently coupled by the hyperfine interaction which, through electron-nuclei flip-flops, produces an oscillation of population between these two levels. This oscillation is interrupted by the irreversible transfer of $S_z = +1/2$ to the optically dressed states. Consequently, both the $S_z = +1/2$ and the $S_z = -1/2$ populations are transferred to $S_z = +5/2$. This mechanism can explain the strong increase of the $S_z = +5/2$ (or $S_z = -5/2$) population for a circularly polarized CW laser excitation slightly detuned around the high or the low energy line of X-Mn.

The spectral width of the pumping signal (i.e., decrease of population obtained on the resonance with the transition) increases with the Rabi energy. Consequently, the optical pumping significantly affects the population trapping mechanism and a more complex dynamics is expected at high excitation intensity [calculation presented in Fig. 7(c) for $\hbar\Omega_R = 50\ \mu$eV, larger than the excitation intensity used in the experiments presented here]. In this high-excitation regime, the population of $S_z = \pm1/2$ is transferred to $S_z = +5/2$ by the population trapping mechanism and simultaneously, the optical pumping empties $S_z = +5/2$. This leads to a transfer from $S_z = +5/2$ and $S_z = \pm1/2$ to $S_z = -3/2$ and $S_z = -5/2$.

In Fig. 8, we report the population of the six spin states of the Mn at fixed Rabi energy $\hbar\Omega_r = 25\ \mu$eV for CW laser detunings around three X-Mn levels: $|J_z = -1, S_z = +1/2\rangle$, $|J_z = -1, S_z = +3/2\rangle$, and $|J_z = -1, S_z = +5/2\rangle$. For each X-Mn level, a strong deviation from the standard optical pumping regime is observed, in agreement with the behavior observed in the experiments presented in Fig. 3. A general trend of these simulations is that the populations of
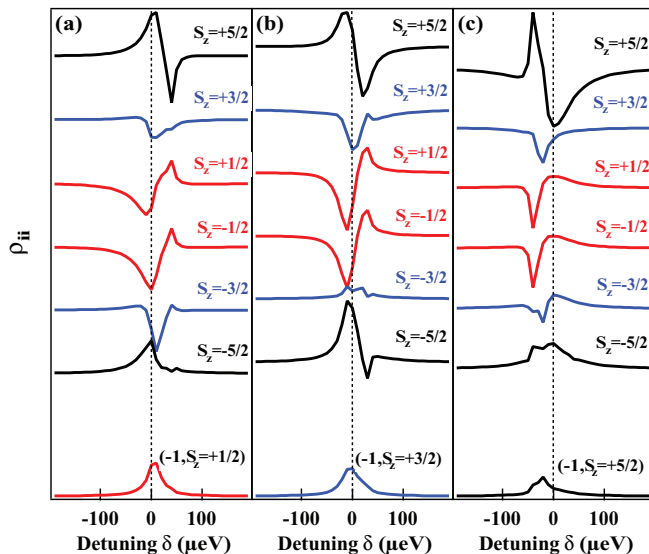
FIG. 8. (Color online) Calculated population of the six spin states of the Mn versus the detuning δ of the CW laser around the X-Mn states $|J_z = -1, S_z = +1/2, I_z\rangle$ (a), $|J_z = -1, S_z = +3/2, I_z\rangle$ (b), and $|J_z = -1, S_z = +5/2, I_z\rangle$ (c) at a fixed Rabi energy $\hbar\Omega_R = 25\ \mu$eV. The relaxation times are $\tau_{Mn} = 250$ ns, $\tau_r = 0.25$ ns, $\tau_{relax} = 60$ ns, $\tau_d = 100$ ps and the Mn fine-structure parameters $\mathcal{D}_0 = 7\ \mu$eV and $E = 0.35\ \mu$eV.

$S_z = +1/2$ and $S_z = -1/2$ always have the same laser detuning dependence. These two states are mixed by the hyperfine coupling with the nuclear spin in an empty dot (Mn alone) and their populations tend to equilibrate as soon as the exciton recombines, whatever the excitation condition are. An excitation on $S_z = +1/2$ also strongly affects the population of $S_z = +5/2$. This is another signature of the coherent coupling between these states induced by the strained anisotropy term E. When the dressed state of $S_z = +1/2$ is on resonance with $S_z = +5/2$ ($\delta > 0$), the population is transferred to $S_z = +1/2$ strongly coupled with $S_z = -1/2$; this is similar to the population trapping mechanism discussed in the case of an excitation on $S_z = +5/2$.

The situation is more complex for an excitation on $S_z = +3/2$ as the standard optical pumping and the population transfer to the optically dressed state can occur simultaneously. The dressed states of $S_z = +3/2$ can be tuned on resonance with the state $S_z = +5/2$ (positive detuning) or with the state $S_z = +1/2$ (negative detuning) for small laser detuning where an efficient optical pumping can take place. For a small negative detuning, an efficient transfer towards the dressed states of $S_z = +3/2$ from $S_z = +1/2$ and $S_z = -1/2$ occurs via flip-flops with the nuclear spin. Simultaneously, the optical pumping empties $S_z = +3/2$. This leads to a transfer of population from $S_z = +3/2$, $S_z = +1/2$, and $S_z = -1/2$ to $S_z = \pm5/2$. This process involves electron nuclei flip-flops and it is expected to take place together with an optical pumping of the Mn nuclear spin. For a positive detuning, a transfer of population occurs from $S_z = +5/2$ to $S_z = +3/2$ via flip-flops with the nuclear spin. The optical pumping tends to empty $S_z = +3/2$ and the population is mainly transferred to $S_z = \pm1/2$.
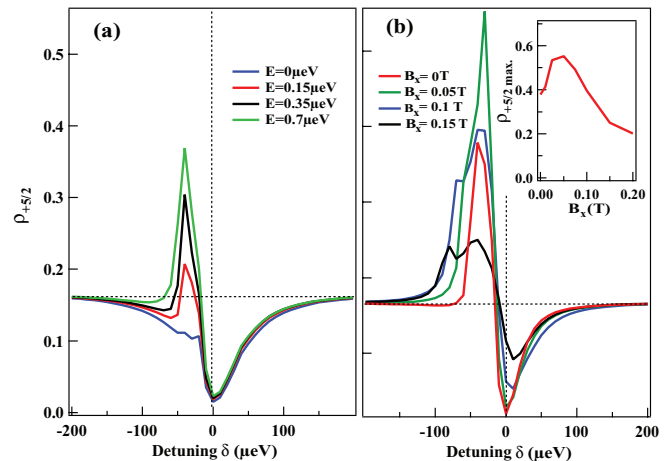

FIG. 9. (Color online) (a) Calculated population of $S_z = +5/2$ versus the CW laser detuning δ around $|J_z = -1, S_z = +5/2, I_z\rangle$: (a) for different values of the in-plane anisotropy of the strain E at a fixed Rabi energy $\hbar\Omega_R = 25\ \mu$eV and (b) for different transverse magnetic field B_x with $E = 0.35\ \mu$eV and $\hbar\Omega_R = 12.5\ \mu$eV. The inset shows the transverse magnetic field dependence of the peak population of $S_z = +5/2$. The relaxation times are $\tau_{Mn} = 250$ ns, $\tau_r = 0.25$ ns, $\tau_{relax} = 60$ ns, $\tau_d = 100$ ps and the magnetic anisotropy $\mathcal{D}_0 = 7\ \mu$eV.

The in-plane strain anisotropy E plays a major role in the population trapping mechanism presented here. This is confirmed by the calculation displayed in Fig. 9(a). In the absence of in-plane strain anisotropy ($E = 0$) the population trapping disappears and the detuning dependence of the Mn spin population is dominated by the standard optical spin pumping mechanism. A value of E corresponding to a few percent of $\mathcal{D}_0$ (5% in the calculation presented in Fig. 7) can explain the characteristic redistribution of population observed in the resonant excitation experiments.

These calculated detuning dependencies explain the non-trivial variation of intensities observed when scanning a CW laser across the overall X-Mn spectrum. Excitation on any Mn spin state mainly affects the population of $S_z \pm 1/2$ and $S_z \pm 5/2$ and the detuning dependence of the Mn spin population always deviates from the standard resonant optical pumping regime.

Since the population trapping relies on the coherent coupling between the Mn spin states, one may wonder how to tune it in order to optimize the spin preparation. One way to control this coupling is by applying a small external magnetic field. As illustrated in Fig. 9(b) a weak in-plane magnetic field induces coherent coupling among the Mn spin states and enhances the population trapping. However, as already observed in optical pumping experiments,[4,17] an equilibrium of the different S_z state populations is restored when the in-plane magnetic field overcomes the magnetic anisotropy independently of the optical excitation conditions, in agreement with the experimental data presented in Fig. 3(c). In the present case, the spin population trapping—and consequently the fidelity of the Mn initialization—is maximum for a transverse magnetic field around 0.05 T.

In addition to the CW laser detuning, its power is another way to control the Mn spin preparation. In the calculated
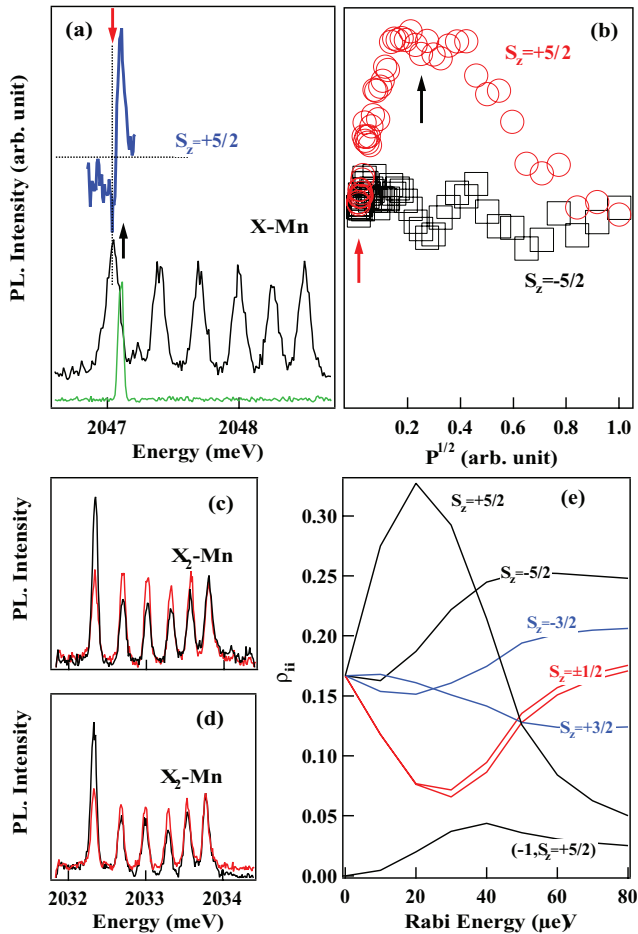
FIG. 10. (Color online) (a) PL of X-Mn in QD3 (black). The green curve is the spectra of the single-mode laser used for the power dependence presented in (b). The blue curve presents the intensity of X_2-Mn for the spin state $S_z = +5/2$ versus the energy of the σ single-mode laser scanned around the low-energy line of X-Mn. (b) PL intensity of the high ($S_z = -5/2$, black squares) and low ($S_z = +5/2$, red circles) energy lines of X_2-Mn versus the square root of the intensity P of the resonant CW laser (quantity proportional to the laser electric field). (c) PL spectra of X_2-Mn for two slightly different excitation energies: excitation energy pointed by the red arrow in (a) (red curve) and by the black arrow in (a) (black curve). (d) PL spectra of X_2-Mn for two different excitation power: excitation power pointed by the red arrow in (b) (red curve) and by the black arrow in (b) (black curve). (e) Calculated power dependence of the different spin states populations for an excitation detuned by $\delta = -40\ \mu$eV from $|J_z = -1, S_z = +5/2, I_z\rangle$. The parameters used in the calculation are $\tau_{\text{Mn}} = 250$ ns, $\tau_r = 0.25$ ns, $\tau_{\text{relax}} = 60$ ns, $\tau_d = 100$ ps, $\mathcal{D}_0 = 7\ \mu$eV, and $E = 0.35\ \mu$eV.

excitation power dependence presented in Fig. 10(e), for a detuning between the pumping laser and the excited transition

$|J_z = -1, S_z = +5/2\rangle$ of $\delta = -40\ \mu$eV, even at low excitation intensity the optically dressed state is on resonance with $S_z = \pm 1/2$. The optical trapping regime already starts at very low excitation intensity. As the excitation intensity increases, the dressed state is shifted away from the $S_z = \pm 1/2$ spin states and the population trapping disappears. A standard optical pumping of the state $S_z = +5/2$ is restored. This nonmonotonic evolution of the population of the resonantly excited level is characteristic of the regime of optical spin population trapping.

A nonmonotonic power dependence is indeed observed in the experiments presented in Fig. 10(b). For a single mode excitation laser detuned on the high-energy side of the state $|J_z = -1, S_z = +5/2\rangle$ [Fig. 10(a)], an increase of the population is observed starting from the low excitation intensity regime. This is the spin population trapping regime. Then the population saturates and decreases at high excitation intensity when the optically dressed state is shifted away from the states $S_z = \pm 1/2$ and the transfer of population is suppressed. Examples of low and high excitation power spectra of X_2-Mn are presented in Fig. 10(d). This experiment confirms that the optical spin population trapping regime can be reached either by changing the laser detuning or by changing the laser excitation intensity.

V. CONCLUSION

In conclusion, we have shown that the coupling with a resonant laser field strongly modifies the spin dynamics of a Mn atom inserted in a strained self-assembled QD. In addition to the standard optical pumping, the Mn spin can be trapped in the state which is optically excited. This mechanism of "spin population trapping" is controlled by the presence of a coherent coupling between the different Mn spin states S_z induced by an in-plane strain anisotropy. Such spin dynamics is not specific to a Mn atom and could be observed in other solid state and atomic spin systems provided that a coherent coupling between the spin sublevels is present. As demonstrated for a Mn atom, the coherent coupling could be induced by a transverse magnetic field.

The population trapping of the Mn electronic spin can also involve flip-flops with the Mn nuclear spin and an optical pumping of the nuclear spin is expected. This optical excitation configuration will be used in future experiments to optically access the nuclear spin of the Mn in its solid state environment. This spin initialization technique could also be extended to QDs containing 2 Mn atoms[32] to optically induce a correlation between the localized spins.

*lucien.besombes@grenoble.cnrs.fr

[1]J. Brossel and F. Bitter, Phys. Rev. **86**, 308 (1952).

[2]M. Atatüre, J. Dreiser, A. Badolato, A. Högele, K. Karrai, and A. Imamoglu, Science **312**, 551 (2006).

[3]B. D. Gerardot, D. Brunner, P. A. Dalgarno, P. Ohberg, S. Seidl, M. Kroner, K. Karrai, N. G. Stoltz, P. M. Petroff, and R. Warburton, Nature (London) **451**, 441 (2008).

[4]C. Le Gall, R. S. Kolodka, C. L. Cao, H. Boukari, H. Mariette, J. Fernandez-Rossier, and L. Besombes, Phys. Rev. B **81**, 245315 (2010).

[5]B. R. Mollow, Phys. Rev. A **5**, 2217 (1972).

[6]G. Jundt, L. Robledo, A. Högele, S. Falt, and A. Imamoglu, Phys. Rev. Lett. **100**, 177401 (2008).

[7]X. Xu, B. Sun, P. R. Berman, D. G. Steel, A. S. Bracker, D. Gammon, and L. J. Sham, Science **317**, 929 (2007).

[8]X. Xu, Bo Sun, E. D. Kim, K. Smirl, P. R. Berman, D. G. Steel, A. S. Bracker, D. Gammon, and L. J. Sham, Phys. Rev. Lett. **101**, 227401 (2008).

[9]M. Kroner, C. Lux, S. Seidl, A. W. Holleitner, K. Karrai, A. Badolato, P. M. Petroff, and R. J. Warburton, Appl. Phys. Lett. **92**, 031108 (2008).

[10]A. Muller, W. Fang, J. Lawall, and G. S. Solomon, Phys. Rev. Lett. **101**, 027401 (2008).

[11]L. Besombes, Y. Leger, L. Maingault, D. Ferrand, H. Mariette, and J. Cibert, Phys. Rev. Lett. **93**, 207403 (2004).

[12]A. Kudelski, A. Lemaitre, A. Miard, P. Voisin, T. C. M. Graham, R. J. Warburton, and O. Krebs, Phys. Rev. Lett. **99**, 247209 (2007).

[13]C. Le Gall, A. Brunetti, H. Boukari, and L. Besombes, Phys. Rev. Lett. **107**, 057401 (2011).

[14]P. Wojnar, C. Bougerol, E. Bellet-Amalric, L. Besombes, H. Mariette, and H. Boukari, J. Crystal Growth **335**, 28 (2011).

[15]A. H. Trojnar, M. Korkusinski, M. Potemski, and P. Hawrylak, Phys. Rev. B **85**, 165415 (2012).

[16]J. Fernandez-Rossier, Phys. Rev. B **73**, 045301 (2006).

[17]C. Le Gall, L. Besombes, H. Boukari, R. Kolodka, J. Cibert, and H. Mariette, Phys. Rev. Lett. **102**, 127402 (2009).

[18]M. Goryca, T. Kazimierczuk, M. Nawrocki, A. Golnik, J. A. Gaj, P. Kossacki, P. Wojnar, and G. Karczewski, Phys. Rev. Lett. **103**, 087401 (2009).

[19]D. E. Reiter, T. Kuhn, and V. M. Axt, Phys. Rev. Lett. **102**, 177403 (2009).

[20]D. E. Reiter, T. Kuhn, and V. M. Axt, Phys. Rev. B **85**, 045308 (2012).

[21]L. Besombes, Y. Leger, J. Bernos, H. Boukari, H. Mariette, J. P. Poizat, T. Clement, J. Fernandez-Rossier, and R. Aguado, Phys. Rev. B **78**, 125324 (2008).

[22]L. Besombes, Y. Leger, L. Maingault, D. Ferrand, H. Mariette, and J. Cibert, Phys. Rev. B **71**, 161307 (2005).

[23]T. Flissikowski, A. Betke, I. A. Akimov, and F. Henneberger, Phys. Rev. Lett. **92**, 227401 (2004).

[24]Additional weak lines are often observed in the photoluminescence of Mn-doped quantum dots. This is a consequence of the coupling with dark exciton states induced by the valence band mixing (Ref. 25).

[25]Y. Leger, L. Besombes, L. Maingault, and H. Mariette, Phys. Rev. B **76**, 045331 (2007).

[26]M. Qazzaz, G. Yang, S. H. Xin, L. Montes, H. Luo, and J. K. Furdyna, Solid State Commun. **96**, 405 (1995).

[27]M. T. Causa, M. Tovar, S. B. Oseroff, R. Calvo, and W. Giriat, Phys. Lett. A **77**, 473 (1980).

[28]L. Cywinski, Phys. Rev. B **82**, 075321 (2010).

[29]C. L. Cao, L. Besombes, and J. Fernandez-Rossier, Phys. Rev. B **84**, 205305 (2011).

[30]M. P. van Exter, J. Gudat, G. Nienhuis, and D. Bouwmeester, Phys. Rev. A **80**, 023812 (2009).

[31]C. Roy and S. Hughes, Phys. Rev. X **1**, 021009 (2011).

[32]L. Besombes, C. L. Cao, S. Jamet, H. Boukari, and J. Fernandez-Rossier, Phys. Rev. B **86**, 165306 (2012).